

# What is the sign of the conductances in crossed Andreev rection?

R. Merlin

Centre de Recherches sur les Très Basses Températures (CRTBT<sup>y</sup>),  
CNRS, BP 166, 38042 Grenoble Cedex 9, France

D. Feinberg

Laboratoire d'Etude des Propriétés Electroniques des Solides (LEPES<sup>z</sup>),  
CNRS, BP 166, 38042 Grenoble Cedex 9, France

Crossed Andreev rection in Ferromagnet / Superconductor / Ferromagnet (FSF) structures is driven by local Andreev rections, which play an important role for transparent enough interfaces and intermediate spin polarizations. This can explain the sign of the crossed conductances in a recent experiments [D. Beckmann et al., cond-mat/0404360]. The effects appear both in the multiterminal hybrid structure model (where phase averaging over the Fermi oscillations is introduced "by hand" within the approximation of a single non-local process) and for finite planar interfaces (where phase averaging naturally results in the microscopic solution with multiple non-local processes).

PACS numbers: 74.50.+r, 74.78.Na, 74.78.Fk

## I. INTRODUCTION

Andreev rection<sup>1</sup> is the mechanism by which charge is transported at normal metal / superconductor (NS) interfaces at voltages below the superconducting gap. A spin-up electron from the N electrode is reflected as a spin-down hole while a Cooper pair is transferred in the superconductor. Andreev rection exists also in ferromagnet / superconductor (FS) junctions but is suppressed as the spin polarization of the ferromagnet increases<sup>2,3,4</sup>. Multiterminal geometries<sup>5,6</sup> have focused an important interest recently. It was shown<sup>7,8,9,10,11,12,13,14,15,16,17</sup> that Andreev rection exists also in FSF junctions where two ferromagnets are connected to a superconductor but can be "non local" in the sense that the incoming spin-up electron and outgoing spin-down hole belong to different electrodes. Non-local Andreev rection is usually called "crossed Andreev rection" (CAR). Elastic cotunneling (EC) is another process by which an electron from one ferromagnet can tunnel through the superconductor and be transmitted in the other ferromagnet, while keeping its spin. Both processes suffer a geometrical reduction with respect to local processes, due to propagation of virtual quasiparticles below the superconducting gap.

Other manifestations of spatially separated pair correlations were obtained in the study of equilibrium properties of FSF trilayers<sup>10,18,19,20,21,22</sup>. It was shown<sup>10,18,19</sup> within a model of multiterminal hybrid structure that the self-consistent superconducting gap can be larger in the parallel alignment. The same result was obtained

for the FSF trilayer with atomic thickness, for half-metal ferromagnets<sup>20</sup> and Stoner ferromagnets<sup>21</sup>. However simulations with a finite thickness<sup>21,22</sup> showed that pair-breaking dominates for strong ferromagnets as the thickness of the superconductor is larger than the Fermi wavelength (with therefore the superconducting gap larger in the antiparallel alignment).

The goal of the theory of crossed Andreev rection is to calculate the conductances of a FSF structure in the parallel and antiparallel alignments. In a first approximation we neglect the dependence of the superconducting gap on the relative spin orientation of the ferromagnets, which is a consistent assumption if the linear size of the contacts is much smaller than the superconducting coherence length. The first approach to this problem was through Landauer formalism<sup>8</sup>. Lowest order perturbation theory<sup>9</sup> gives an interpretation in terms of CAR and EC processes. The effect of non-collinear ferromagnets was also investigated<sup>12,13</sup>, with the aim of describing transport of Cooper pairs at the interface between a superconductor and a ferromagnet containing a domain wall. The Josephson effect between two superconductors connected by two spatially separated conduction channels was also examined<sup>12</sup> and it was found that there is no Josephson effect within lowest order perturbation theory unless the length of the ferromagnets is smaller than the elastic mean free path, a condition that is not usually verified in experiments. Toy models for more complicated geometries involving Aharonov-Bohm effects related to crossed correlations were also investigated<sup>14</sup>. Disorder effects were also discussed recently for tunnel interfaces<sup>13,15</sup> and it was found that the geometrical reduction is less severe in the presence of disorder in the superconductor (dirty limit). Another geometry with a normal metal island connected to one superconductor and two ferromagnets was proposed in Ref. 16. Noise correlations were also discussed recently within lowest order perturbation theory<sup>17</sup>.

CAR and EC were probed in a recent experiment by

merlin@grenoble.cnrs.fr

<sup>y</sup>U.P.R. 5001 du CNRS, Laboratoire conventionné avec l'Université Joseph Fourier

<sup>z</sup>U.P.R. 11 du CNRS, Laboratoire conventionné avec l'Université Joseph Fourier

Beckmann et al.<sup>23</sup>. The overall experimental results are in agreement with theory except for the sign of the current: it was predicted theoretically<sup>7,9</sup> that for tunnelbarriers the currents in the parallel and antiparallel spin orientations have an opposite sign whereas in experiments<sup>23</sup> they have the same sign. We resolve here this apparent contradiction by noting that the large interface transparencies used in experiments imply that the non local CAR and EC processes are "dressed" by local Andreev reactions at the two FS interfaces. This dressing is easily transcribed in terms of a perturbative expansion for the Keldysh Green's functions. Due to the strong damping of quasiparticles in the superconductor, a reasonable approximation involves a single non local propagator while local ones are treated to all orders. We also carry out numerical simulations for infinite planar interfaces in which multiple non local processes are taken into account and find a good agreement with the analytical approach.

The article is organized as follows. Preliminaries are given in section II. The properties of multiteminal hybrid structures are investigated in section III. Infinite planar interfaces are investigated in section IV. Concluding remarks are given in section V.

## II. PRELIMINARIES

In this section we provide the form of the Green's functions and Hamiltonians that we use throughout the article.

### A. Hamiltonians

The superconductor is described by the BCS Hamiltonian<sup>24</sup>:

$$H_{BCS} = \sum_{k_x} \langle k \rangle c_{k_x}^\dagger c_{k_x} + \sum_{k_x} \langle c_{k_x}^\dagger c_{k_x}^\dagger c_{k_x} c_{k_x} \rangle; \quad (1)$$

where  $\langle k \rangle = \sim^2 k^2 = 2m$  is the free electron dispersion relation and the superconducting gap. The ferromagnets are described by the Stoner model

$$H_{Stoner} = \sum_{k_x} \langle k \rangle c_{k_x}^\dagger c_{k_x} + \sum_{k_x} h_{ex} \langle c_{k_x}^\dagger c_{k_x}^\dagger c_{k_x} c_{k_x} \rangle; \quad (2)$$

where  $h_{ex}$  is the exchange field.

### B. Green's functions in reciprocal space

In the absence of non collinear magnetizations the Nambu representation corresponds to two  $2 \times 2$  matrices,

one in the sector  $S_z = 1=2$  and the other in the sector  $S_z = -1=2$  ( $S_z$  is the projection of the spin along the quantization axis chosen parallel to the exchange field). The advanced Green's function in the sector  $S_z = 1=2$  is given by

$$g_{x,y}^A(t; t^0) = i(t - t^0) \quad (3)$$

$$hfc_{x,y}^A(t; c_{x,y}^+, t^0)gi hfc_{x,y}^A(t; c_{x,y}^-, t^0)gi \\ hfc_{x,y}^A(t; c_{x,y}^+, t^0)gi hfc_{x,y}^A(t; c_{x,y}^-, t^0)gi;$$

where  $x$  and  $y$  are two arbitrary sites and  $gi$  is an anticommutator. Using the Hamiltonian (1) we obtain the advanced Green's function in reciprocal space<sup>25</sup>:

$$g_{1,1}^{1,1,A}(\epsilon; \epsilon_s) = \frac{u_k^2}{\epsilon - E_k - i\epsilon_s} + \frac{v_k^2}{\epsilon + E_k - i\epsilon_s} \quad (4)$$

$$f_{1,2}^{1,2,A}(\epsilon; \epsilon_s) = \frac{1}{[\epsilon - E_k - i\epsilon_s][\epsilon + E_k - i\epsilon_s]}; \quad (5)$$

where  $\epsilon = \sim^2 k^2 = 2m$ ,  $F$  is the Fermi energy with respect to the Fermi level  $\epsilon_F = \sim^2 k_F^2 = 2m$ ,  $E_k = \epsilon^2 + \frac{\Delta^2}{k^2}$  is the quasiparticle energy,  $u_k^2 = (1 + \epsilon_k = E_k) = 2$  and  $v_k^2 = (1 - \epsilon_k = E_k) = 2$  are the BCS coherence factors, and  $\epsilon_s$  is a small parameter related to inelastic processes in the superconductor (a typical value in experiments is  $\epsilon_s = 10^{-2}$ <sup>26,27</sup>).

The "11" component of the Green's function of a ferromagnet is given by

$$g_{a,a}^{1,1}(\epsilon; \epsilon_s) = \frac{1}{\epsilon + h_{ex} - iF}; \quad (6)$$

and a similar expression is obtained for  $g_{a,a}^{2,2}$ . The parameter  $F$  can be large in a ferromagnet (for instance  $F$  is estimated to be 300 K in the magnetic alloy CuNi<sup>28</sup>).

### C. Green's functions in real space

The local Green's functions of a superconductor take the form

$$g_{\pm} = g_{\pm} = \frac{s}{2 - \frac{\epsilon}{\Delta^2}} \quad (7)$$

where  $s$  is the normal state density of state,  $\epsilon$  is the energy with respect to the Fermi level and  $\Delta$  is the superconducting gap. The non local Green's functions of the superconductor take the form

$$g_{\pm} = \frac{s}{k_F R} \exp \left( \frac{R}{\epsilon} \right) \frac{\sin(k_F R)}{\frac{P}{2} - \frac{\epsilon}{\Delta^2}} \quad (8)$$

$$+ \cos(k_F R) \frac{1}{0} \frac{0}{1};$$

where  $\epsilon = \sim v_F = \frac{P}{2} - \frac{\epsilon}{\Delta^2}$  is the BCS coherence length. The local Green's functions of the ferromagnet is given by

$$g_{a,a} = i \begin{pmatrix} a^+ & 0 \\ 0 & a^- \end{pmatrix}; \quad (9)$$

where  $a_{\alpha}^{\uparrow}$  and  $a_{\alpha}^{\downarrow}$  correspond to the spin-up and spin-down density of states in the ferromagnet  $\alpha$ . A spin polarization  $P$  corresponds to  $a_{\alpha}^{\uparrow} = \frac{1}{2} (1 + P_{\alpha})$  and  $a_{\alpha}^{\downarrow} = \frac{1}{2} (1 - P_{\alpha})$ .

#### D. Mixed Green's functions

To describe infinite planar contacts we use Green's functions parameterized by the distance  $R$  along the  $z$  axis and the two wave-vectors  $k_x$  and  $k_y$ . This parameterization is well suited for a situation where translation invariance holds in the  $(x, y)$  plane parallel to the interface but not in the  $z$  direction perpendicular to the interface. The kinetic energy is separated into the sum of  $k = \sqrt{k_x^2 + k_y^2} = 2m_F$  and  $k_z = \sqrt{k_z^2} = 2m$ . After a Fourier transform with respect to  $k_z$  we obtain

$$\hat{g}^A(R; \alpha; k) = \frac{P}{2\omega} \frac{1}{2m a_0^2} \exp(ik_z R) \begin{pmatrix} \frac{1}{i \frac{P}{2} - (\alpha - i\omega)^2} & & & \\ & \frac{1}{i \frac{P}{2} - (\alpha - i\omega)^2} & & \\ & & \frac{1}{i \frac{P}{2} - (\alpha - i\omega)^2} & \\ & & & \frac{1}{i \frac{P}{2} - (\alpha - i\omega)^2} \end{pmatrix} + i \begin{pmatrix} 1 & 0 \\ 0 & 1 \end{pmatrix}; \quad (10)$$

with

$$k_z = \frac{P}{2m} \frac{1}{i \frac{P}{2} - (\alpha - i\omega)^2} \quad (11)$$

where  $a_0$  in Eq. (10) is the lattice parameter.

The mixed Green's function of a ferromagnet is given by

$$\hat{g}_{1;1}^A(R; \alpha; k) = \frac{P}{2\omega} \frac{1}{2m a_0^2} \exp(ik_z R) \begin{pmatrix} & & & \\ & \frac{1}{i \frac{P}{2} + i\omega + h_{\text{ex}}} & & \\ & & \frac{1}{i \frac{P}{2} + i\omega + h_{\text{ex}}} & \\ & & & \frac{1}{i \frac{P}{2} + i\omega + h_{\text{ex}}} \end{pmatrix} \quad (12)$$

with

$$k_z = \frac{P}{2m} \frac{1}{i \frac{P}{2} + i\omega + h_{\text{ex}}} \quad (13)$$

#### E. Transport properties

The Green's functions  $\hat{G}_{ij}$  of the connected system are obtained by solving the Dyson equation. In a compact notation the Dyson equation takes the form  $\hat{G} = \hat{g} + \hat{g} \hat{G} \hat{g}$ , where  $\hat{G}$  is the self-energy corresponding to the tunnel Hamiltonian,  $\hat{g}$  is a summation over spatial variables and a convolution over time variables, and  $\hat{g}$  is the Green's function of the disconnected system with  $\hat{g} = 0$ .

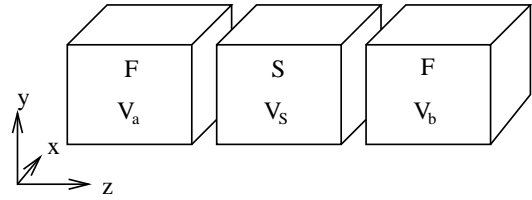


FIG. 1: Schematic representation of the Andreev reflection geometry in a FSF structure. We have  $V_a = V_s = 0$ ,  $V_b \neq 0$ . The sites of the superconductor corresponding to the contact with electrode "a" ("b") are labeled by "a" ("b").

Transport properties<sup>27,29</sup> are obtained by evaluating the Keldysh Green's function

$$\hat{G}^+ = [\hat{f} + \hat{G}^R \hat{f}] \hat{g}^+; \quad \hat{f} + \hat{G}^A \hat{f}; \quad (14)$$

The spin-up current through the link  $a$  is given by

$$I = \frac{e}{2h} \int d^2k \text{Tr} \left[ \hat{f}_a \hat{G}_{;a}^+ (\alpha) \hat{f}_{;a} \hat{G}_{;a}^+ (\alpha) \hat{G}^A \right] + (h_{\text{ex}} \alpha - h_{\text{ex}}); \quad (15)$$

where the trace is a summation over the "11" and "22" components of the Green's function in the Nambu representation, and  $\hat{G}^A$  is one of the Pauli matrices. The term  $(h_{\text{ex}} \alpha - h_{\text{ex}})$  corresponds to a summation over the "33" and "44" components in the 4x4 Nambu representation<sup>12</sup> in the sector  $S_z = \pm 1/2$ . For a normal metal the four components of the current are equal and we recover the usual form of the transport formula<sup>27,29</sup>.

### III. MULTITERMINAL HYBRID STRUCTURES

#### A. Transport formula

We start with the Andreev reflection geometry on Fig. 1. In the Hamiltonian approach, the exact geometry is unimportant: the results are the same for two lateral contacts (like in the experiment<sup>23</sup>) or opposite contacts (Fig. 1). The total current owing between the two electrodes is the sum of two contributions: i) the CAR current (Andreev process) circulating from both electrodes "a" and "b", and ii) the EC current owing from "a" to "b". Those are given by

$$\begin{aligned} I_{\text{CAR}}(V_a, V_b) &= 2 \frac{t_a^2 t_b^2 e}{h} \frac{a_{\alpha}^{\uparrow} b_{\alpha}^{\downarrow}}{a_{\alpha}^{\downarrow} b_{\alpha}^{\uparrow}} \\ &+ \frac{d!}{eV_b} \frac{G^{1/2;A}(\alpha) G^{2;1;R}(\alpha)}{eV_a} \\ &+ 2 \frac{t_a^2 t_b^2 e}{h} \frac{a_{\alpha}^{\downarrow} b_{\alpha}^{\uparrow}}{a_{\alpha}^{\uparrow} b_{\alpha}^{\downarrow}} \\ &+ \frac{d!}{eV_b} \frac{G^{2;1;A}(\alpha) G^{1/2;R}(\alpha)}{eV_a}; \end{aligned} \quad (16)$$

and

$$\begin{aligned} I_{EC}(V_a; V_b) &= 2 \frac{2t_a^2 t_b^2 e}{h} \delta_{ab} + \frac{d! G^{1;1;A} (!) G^{1;1;R} (!)}{eV_a eV_b} \\ &+ 2 \frac{2t_a^2 t_b^2 e}{h} \delta_{ab} + \frac{d! G^{2;2;A} (!) G^{2;2;R} (!)}{eV_b eV_a} \end{aligned} \quad (17)$$

The crossed conductance is defined as  $G_{ab}(V_a; V_b) = \mathbb{E} I_a, (V_a; V_b) = \mathbb{E} V_b$ , where  $I_a, (V_a; V_b) = I_{CAR}(V_a; V_b) + I_{EC}(V_a; V_b)$  is the total crossed current through the link  $a$ . The crossed conductance can be expressed in terms of the spin polarizations  $P_a$  and  $P_b$ :

$$G_{ab} = 4 \frac{2t_a^2 t_b^2 e}{h} F_a F_b f \quad (18)$$

$$(1 - P_a P_b) \frac{G^{1;2;A} (eV_b) G^{2;1;R} (eV_b)}{(1 + P_a P_b) G^{1;1;A} (eV_b) G^{1;1;R} (eV_b)} \quad (19)$$

$$+ (eV_b - eV_a) g \quad (20)$$

Averaging over the Fermi oscillations<sup>9,11</sup> is used to simulate an extended contact as the sum of channels in parallel with a distribution of length  $R$ :

$$\begin{aligned} \frac{Z}{G^{1;2;A} (!) G^{2;1;R} (!)} &= \frac{1}{R} \int_{R/2}^{R+R/2} dR \quad (21) \\ G^{1;2;A} (R; !) G^{2;1;R} (R; !); \end{aligned}$$

with  $R = F = 2 = k_F$ .

The tunneling limit involves bare Green's functions, which satisfy  $g^{1;2;A} (!) g^{2;1;R} (!) = g^{1;1;A} (!) g^{1;1;R} (!)$ , therefore the crossed conductances for parallel ( $P_a = P_b$ ) and antiparallel ( $P_a = -P_b$ ) spin polarizations are opposite. This is not necessarily true for transparent interfaces, where dressing of the quasiparticle propagators occurs in the superconductor.

## B. Perturbative expansion in $1=(k_F R)$

Now we revisit the perturbative expansion<sup>9,11,12</sup> used to describe crossed Andreev reflection. We suppose that the contacts  $a$ - and  $b$ - are highly transparent so that multiple Andreev reflections take place locally. However  $k_F R$  is large so that in a first approximation a single non local process is included in  $\hat{G}^0$ . This leads to

$$\hat{G}^0, = \hat{M}^{(0)} \hat{g}^0, \hat{N}^{(0)} ; \quad (22)$$

where  $\hat{M}^{(0)} (, \hat{N}^{(0)} ,)$  describes the dressing by multiple Andreev reflections at the contact  $a$ - ( $b$ -).  $\hat{M}^{(0)} ,$  is determined by the equation  $\hat{G}^{(0)} , = \hat{M}^{(0)} \hat{g}^0, ,$  where  $\hat{G}^{(0)} ,$

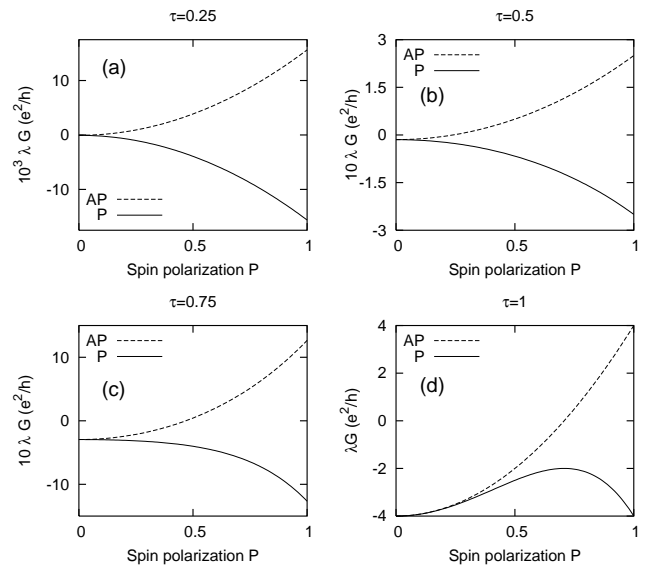


FIG. 2: Variation of the normalized linear crossed conductances  $G_P$  (P) (solid line) and  $G_{AP}$  (P) (dashed line) as a function of the spin polarization  $P$ , for  $\tau = 0.25$  (a),  $\tau = 0.5$  (b),  $\tau = 0.75$  (c),  $\tau = 1$  (d). Note the different scaling factors on the conductance axis. and  $\tau = 1$

is the fully dressed propagator at site with  $t_b, = 0$ . We find easily

$$\hat{M}^{(0)} ; = \hat{I}^h \hat{g}^0, \hat{t}_{;a} \hat{g}_{a;a} \hat{t}_{;a}^i \quad (23)$$

$$\hat{N}^{(0)} ; = \hat{I}^h \hat{t}_{;b} \hat{g}_{b;b} \hat{t}_{;b}^i \hat{g}^0, \quad (24)$$

Generalizing Ref. 9 we evaluate the phase averaging of the following Green's functions:

$$\overline{g^{1;1}}^2 = \overline{g^{2;2}}^2 = \overline{g^{1;2}}^2 \quad (25)$$

$$= \frac{2}{2} \frac{2}{2} \frac{S}{(k_F R)^2} \exp \frac{2R}{(1)} \frac{2}{2} \frac{!^2}{!^2} \quad (26)$$

$$\overline{g^{1;1} g^{2;2}} = \frac{2}{2} \frac{2}{2} \frac{S}{(k_F R)^2} \exp \frac{2R}{(1)} \frac{2}{2} \frac{!^2}{!^2} \quad (27)$$

$$\overline{g^{1;1} g^{1;2}} = \frac{2}{2} \frac{2}{2} \frac{S}{(k_F R)^2} \exp \frac{2R}{(1)} \frac{!}{2} \frac{!^2}{!^2} \quad (28)$$

We use Eqs. (25)–(27) and Eq. (22) to evaluate the phase averaged Green's function in the CAR and EC currents given by (16) and (17).

## C. Crossed conductance in a FSF structure

### 1. Normalization of the tunnel amplitudes

For a NN contact, highly transparent interfaces correspond to  $t = t_0$ , where  $t_0$  is such that  $2t_0^2 = 1$ . The

NN contact conductance is given by  $G_{NN} = (2e^2/h)$ , with<sup>27</sup>

$$= \frac{4(t=t_0)^2}{(1+(t=t_0)^2)^2} \quad (28)$$

The conductance of a NF contact is given by  $G_{NF} = (e^2/h)(\# + \#)$ , with

$$\# = \frac{4^2 t^2_{NF} (1+P)}{[1+2t^2_{NF} (1+P)]^2} \quad (29)$$

$$\# = \frac{4^2 t^2_{NF} (1-P)}{[1+2t^2_{NF} (1-P)]^2} \quad (30)$$

The value  $t_0$  of  $t$  corresponding to a perfect transmission in the spin-up channel is given by

$$2t_0^2(P)_{NF} (1+P) = 1 \quad (31)$$

The conductance of a SF contact with perfect transmission in the spin-up channel ( $t = t_0(P)$ ) is given by

$$G_{NF} = \frac{e^2}{h} \frac{B}{C} \frac{1}{1 + \frac{4 \frac{1-P}{1+P}}{1 + \frac{1-P}{1+P}}} \quad (32)$$

varying between  $e^2/h$  for half-metal ferromagnets and  $2e^2/h$  in the absence of spin polarization. In the following we normalize the hopping amplitude  $t$  to the maximal value  $t_0(1)$  of  $t_0(P)$ :  $t = t_0(1)$ , with between 0 and 1.

## 2. Linear crossed conductance

The linear crossed conductances are given by

$$G_{AP} = \frac{4e^2}{h} \frac{4}{D^2(P)} - \frac{4(1-P^2)}{D^2(P)} + P^2 \quad (33)$$

$$G_P = \frac{4e^2}{h} \frac{4}{D^2(P)} - \frac{4(1-P^2)(1-2P^2)}{D^2(P)} - P^2 \quad ; \quad (34)$$

with  $D(P) = 1 + 4(1-P^2) = 4$ , and  $= 2(k_F R)^2 \exp(2R = 0)$  in the ballistic limit, and  $= 2(k_F l_e)(k_F R) \exp(2R = 0)$  in the diffusive limit<sup>15</sup>, where  $l_e$  is the elastic mean free path and  $0$  the coherence length at zero energy. The variations of  $G_{AP}(P)$  and  $G_P(P)$  are shown on Fig. 2 for increasing values of  $P$ . We obtain  $G_{AP}(P) \neq G_P(P)$  for small values of  $P$  ( $P = 0.25$  on Fig. 2-(a)). As  $P$  is increased  $G_{AP}(P)$  changes sign as shown on Figs. 2-(b), 2-(c) and 2-(d). For half-metal ferromagnets we have  $G_{AP}(P) = G_P(P)$  for all values of  $P$ , as it can be seen from Eqs. (33) and (34).

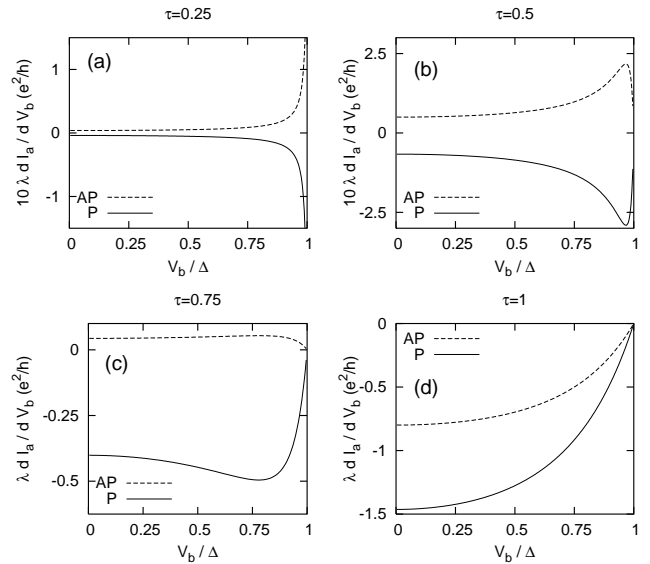


FIG. 3: Variation of the normalized crossed conductance  $(V_b)G(V_b) = \partial I_a / \partial V_b (V_a = 0; V_b)$  as a function of the normalized voltage  $V_b =$ , for  $P = 0.5$  and increasing values of the dimensionless tunnel amplitude  $t$ . The parallel (antiparallel) alignment corresponds to the solid (dashed) line

## 3. Crossed conductance versus voltage

The variations of the crossed conductances as a function of the voltage  $V_b$  applied on electrode "b" are shown on Fig. 3 for  $P = 0.5$ . For small interface transparencies ( $= 0.25$  and  $= 0.5$ ) the crossed conductances in the parallel and antiparallel alignments are approximately opposite in the entire voltage range. The crossed conductance at  $V_b =$  is vanishingly small, both in the parallel and antiparallel alignments and for arbitrary spin polarizations.

For half-metal ferromagnets the crossed conductances take the form

$$(V_b)G_{AP}(V_b) = (V_b)G_P(V_b) = \frac{4}{4 - \frac{2}{V_b^2}} \frac{2}{1 + \frac{4}{2} \frac{V_b^2}{V_b^2}} \quad ; \quad (35)$$

where  $(V_b)$  has the same expression as except that  $0$  is replaced by the coherence length at a finite energy  $0 = \frac{4}{2} \frac{V_b^2}{V_b^2}$ . Eq. (35) is approximately equal to  $(8 = 4)(1 - V_b^2)$  if  $! = 4$ , and approximately equal to  $4 \frac{4}{2} = (\frac{2}{2} \frac{V_b^2}{V_b^2})$  if  $V_b = 4$ . For small there is thus a maximum in the crossed conductance<sup>11</sup> at a voltage  $V_b = (1 - 4 = 2)$ . This argument for  $P = 1$  is compatible with the behavior of the crossed conductances for  $V_b = 1$  and  $P = 0.5$  on Fig. 3.

#### 4. Crossed conductance of a FSN or NSF junction

The linear crossed conductance of a FSN junction

$$G = \frac{e^2}{h} \frac{8^8 (1 - P^2)}{(1 + 4^4 (1 - P^2) = 4) (1 + 4^4 = 4)} \quad (36)$$

is proportional to  $P^8$  and thus very small for tunnel interfaces. However it can take measurable values for highly transparent interfaces and with a weakly polarized ferromagnet or even a normal metal.

#### D. Interpretation of the dressing by local processes

One of the terms contributing to  $G_{\parallel}^{1;1;A} G_{\parallel}^{1;1;A}$  in the parallel alignment is

$$M_{\parallel}^{(0);1;2} g_{\parallel}^{2;1} N_{\parallel}^{(0);1;1} M_{\parallel}^{(0);1;2} g_{\parallel}^{2;1} N_{\parallel}^{(0);1;1}; \quad (37)$$

from which we deduce one of the terms of order  $t_a^4 t_b^4$  contributing  $t_a^2 t_b^2$  to  $G_{\parallel}^{1;1;A} G_{\parallel}^{1;1;A}$ :

$$t_{\parallel a}^{1;1} t_{\parallel a}^{1;1} t_{\parallel a}^{1;1} g_{\parallel a}^{1;2} t_{\parallel a}^{2;2} g_{\parallel a}^{2;2;A} t_{\parallel a}^{2;2} g_{\parallel a}^{2;1}; \quad (38)$$

$$t_{\parallel b}^{1;1} t_{\parallel b}^{1;1} t_{\parallel b}^{1;1} g_{\parallel b}^{1;2} t_{\parallel b}^{2;2} g_{\parallel b}^{2;2;B} t_{\parallel b}^{2;2} g_{\parallel b}^{2;1}; \quad (39)$$

This process corresponds to a diagram in which a spin-up electron from electrode 'a' is locally Andreev reflected as a spin-down hole that makes an excursion in electrode 'a', is converted in a spin-up electron in electrode 'b' through a non local Andreev reflection. The spin-up electron in electrode 'b' undergoes a local Andreev reflection, is converted in a spin-down hole that is transformed in a spin-up electron by a non local Andreev reflection. This process is not possible for halfmetal ferromagnets, in which case the linear conductance is equal to the bare conductance, proportional to  $t^4$ .

#### IV. INFINITE PLANAR INTERFACES WITH A BULK SUPERCONDUCTOR

Now we consider infinite planar 2D interfaces connecting a bulk 3D superconductor to bulk 3D ferromagnets. Within this approach we do not have to impose 'by hand' phase averaging as we did in the previous section (see Eqs. (25)–(27)). We use the mixed Green's functions introduced in section II D. The evaluation of the integrals in the expression of the CAR and EC currents is briefly described in Appendix A. A realistic model would involve an estimate of the inverse proximity effect, i.e. how the superconducting gap depends on the relative spin orientation of the ferromagnetic electrodes<sup>18,19,20,21,22</sup>. Here we consider the infinite planar limit just as a test of the approach in the preceding section and do not impose self-consistency on the superconducting gap.

We calculate the crossed current through electrode 'a' with a finite voltage  $V_b$  on electrode 'b', and with  $V_a = 0$

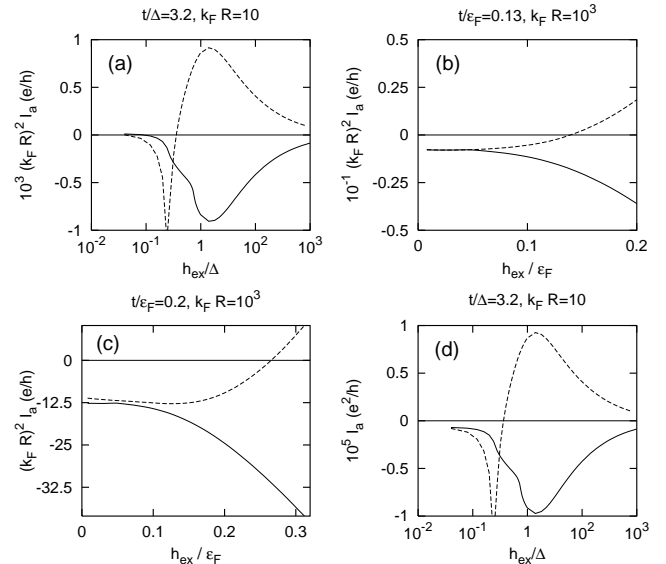


FIG. 4: Variation of the total current  $I_a$  through electrode 'a' evaluated with  $eV_a = 0$  and  $eV_b = -2$  as a function of the exchange field, with  $t = \epsilon_F = 4 \cdot 10^{-3}$ . The parallel (antiparallel) alignment corresponds to the solid (dashed) line. (a), (b) and (c) correspond to a full Green's function calculation with the non local processes at all orders. (d) corresponds to the approximation given by Eq. (22). We use  $s = 10^{-1}$  and  $\epsilon_F = 0.4$  but obtained similar results for  $\epsilon_F = 10^{-1}$ .

and suppose that the distance between the ferromagnets is much larger than the Fermi wavelength. The variations of the current evaluated at  $V_b = -2$  as a function of  $h_{\text{ex}} =$  is shown on Fig. 4 for different values of the distance  $R$  between the contacts. For small values of  $t =$  we obtain one Andreev bound state for weak ferromagnets for which  $h_{\text{ex}}$  and  $t$  have the same order of magnitude (see Fig. 4-(a)). Andreev bound states for weak ferromagnets were already discussed elsewhere<sup>22</sup>. For larger values of  $t =$  and larger values of  $R = a_0$  (see Fig. 4-(b)) we obtain  $I_{AP} \neq I_p$  up to relatively large values of  $h_{\text{ex}} =$  and  $I_{AP} \neq I_p$  for the largest values of  $h_{\text{ex}} =$ . The overall variation on Fig. 4-(a), Fig. 4-(b) and Fig. 4-(c) looks like Fig. 2-(a). Fig. 4-(d) corresponds to the same parameters as Fig. 4-(a) except that we used the approximation (22) of a single non local Andreev reflection on Fig. 4-(d) whereas Fig. 4-(a) was obtained without approximation. The two variations are almost identical, except for the regime  $h_{\text{ex}} =$ . The agreement is even better for larger values of  $R$  (not shown on Fig. 4). This illustrates the validity of the approximation (22) in which we keep a single non local Andreev reflection.

#### V. CONCLUSIONS

To conclude we have proposed an explanation to the signs of the crossed currents in the recent experiment

by Beckmann et al<sup>23</sup>. For small interface transparencies we recover the results of perturbation theory to order  $t_a^2 t_b^2$  (the crossed conductance in the parallel alignment is opposite to the crossed conductance in the antiparallel alignment). For larger interface transparencies the propagators of crossed Andreev reflection and elastic cotunneling are "dressed" by local Andreev reflections. As a result the crossed conductance in the antiparallel alignment can change sign as the interface transparencies are increased. We also carried out simulations of finite planar interfaces and found the same qualitative behavior without imposing phase averaging by hand and without using the approximation in which a single non-local process is kept while local processes are treated to all orders.

#### Acknowledgments

One of the authors (D.F.) acknowledges stimulating discussions with G. D. Dautscher and F. Sols.

#### APPENDIX A: EVALUATION OF INTEGRALS FOR FINITE PLANAR INTERFACES

In this Appendix we give necessary technical details regarding changes of variable for evaluating the current with finite planar interfaces. The "11" component of the CAR current takes the form

$$I_{1;1}^{\text{CAR}} = 4 \frac{3t_a^2 t_b^2 e}{h} \frac{2m a_0^2}{\sim^2} \frac{Z_{eV_a}}{d!} \frac{Z_D}{d} \frac{a_{1;1}^a (! eV_a; k)}{a_{2;2}^b (! eV_b; k)} G_{1;2}^A; ;^2 \quad (\text{A } 1)$$

and the "11" component of the EC current takes the form

$$I_{1;1}^{\text{EC}} = 4 \frac{3t_a^2 t_b^2 e}{h} \frac{2m a_0^2}{\sim^2} \frac{Z_{eV_a}}{d!} \frac{Z_D}{d} \frac{a_{1;1}^a (! eV_a; k)}{a_{1;1}^b (! eV_b; k)} G_{1;1}^A; ;^2 \quad (\text{A } 2)$$

Similar expressions are obtained for the "22" currents and for the currents in the spin-down sector.

The density of state  $a_{1;1}^a (! eV_a; k)$  and  $a_{1;1}^b (! eV_b; k)$  deduced from Eq. 12 contain a square root singularity. For instance

$$a_{1;1}^a (! eV_a; k) = \frac{P}{\sim} \frac{\sqrt{2m a_0^2}}{P} \frac{(! eV_a}{! eV_a} \frac{k + h_a}{k + h_a} \quad (\text{A } 3)$$

After a change of variable  $I_{1;1}^{\text{CAR}}$  takes the form

$$I_{1;1}^{\text{CAR}} = 8 \frac{3t_a^2 t_b^2 e}{h} \frac{2m a_0^2}{\sim^2} \frac{Z_{x_{\text{max}}}}{x_{\text{min}}} \frac{Z_{u_{\text{max}}}}{dx} \frac{du}{2x + u^2} G_{1;2}^A; (! (x); k) \quad (\text{A } 4)$$

where explicit expressions of  $x (!)$ ,  $x_{\text{min}}$ ,  $x_{\text{max}}$  and  $u_{\text{max}}$  can be obtained in each case. For instance if  $eV_b < eV_a$  we have  $x (!) = ! + e(V_a + V_b) = 2(h_a + h_b) = 2$  and  $u = \frac{P}{!} \frac{du}{eV_a} \frac{k + h_a}{k + h_a}$ . The integral (A 4) is then evaluated by making the changes of variable  $v^2 = 2x$  and  $(u; v) = (\cos \theta; \sin \theta)$ , therefore absorbing the square root singularity in a change of variable.

<sup>1</sup> A. F. Andreev, Zh. Eksp. Teor. Fiz. 46, 1823 (1964) [Sov. Phys. JETP 19, 1228 (1964)].

<sup>2</sup> M. J. M. de Jong and C. W. J. Beenakker, Phys. Rev. Lett. 74, 1657 (1995).

<sup>3</sup> R. J. Soulen et al., Science 282, 85 (1998).

<sup>4</sup> S. K. Upadhyay et al., Phys. Rev. Lett. 81, 3247 (1998).

<sup>5</sup> C. J. Lambert and R. R. Aminondi, J. Phys.: Condens. Matter 10, 901 (1998).

<sup>6</sup> F. J. Jedema, B. J. van Wees, B. H. Hoving, A. T. F. Filip and T. M. Klapwijk, Phys. Rev. B 60, 16549 (1999).

<sup>7</sup> C. J. Lambert, J. Koltai, and J. Cserti, in Towards the controllable quantum states (Mesoscopic superconductivity and spintronics, p. 119, Eds H. Takayanagi and J. Nitta, World Scientific (2003)).

<sup>8</sup> G. D. Dautscher and D. Feinberg, App. Phys. Lett. 76, 487 (2000).

<sup>9</sup> G. Falci, D. Feinberg, and F. W. J. Heijking, Europhysics Letters 54, 255 (2001).

<sup>10</sup> R. M. Elin, J. Phys.: Condens. Matter 13, 6445 (2001);

<sup>11</sup> R. M. Elin and D. Feinberg, Eur. Phys. J. B 26, 101 (2002).

<sup>12</sup> R. M. Elin and S. Peysson, Rev. B 68, 174515 (2003).

<sup>13</sup> N. M. Chtchelkatchev, I. S. Burmistrov, Phys. Rev. B 68,

140501 (2003).

<sup>14</sup> R. M. Elin, H. Jirari and S. Peysson, J. Phys.: Condens. Matter 15, 5591 (2003).

<sup>15</sup> D. Feinberg, Eur. Phys. J. B 36, 419 (2003).

<sup>16</sup> D. Sanchez, R. Lopez, P. Samuelsson and M. Buttiker, Phys. Rev. B 68, 214501 (2003).

<sup>17</sup> G. Bignon, M. Houzet, F. Pistolesi, and F. W. J. Heijking, cond-mat/0310349.

<sup>18</sup> V. Apinyan and R. M. Elin, Eur. Phys. J. B 25, 373 (2002).

<sup>19</sup> H. Jirari, R. M. Elin and N. Stefanakis, Eur. Phys. J. B 31, 125 (2003).

<sup>20</sup> A. Buzdin and M. Daumens, Europhys. Lett. 64, 510 (2003).

<sup>21</sup> R. M. Elin and D. Feinberg, Europhys. Lett. 65, 96 (2004).

<sup>22</sup> R. M. Elin, Eur. Phys. J. B 39, 249 (2004).

<sup>23</sup> D. Beckmann, H. B. Weber and H. v. Lohneysen, cond-mat/0404360.

<sup>24</sup> M. Tinkham, Introduction to superconductivity, Second Edition, McGraw-Hill (1996).

<sup>25</sup> A. A. Abrikosov, L. P. Gor'kov, and I. E. Dzyaloshinski, Methods of quantum field theory in statistical physics, Dover (1975).

<sup>26</sup> S.B. Kaplan et al, *Phys. Rev. B* **14**, 4854 (1976).

<sup>27</sup> J.C. Cuevas, A. Martínez-Rodero and A. Levy Yeyati, *Phys. Rev. B* **54**, 7366 (1996).

<sup>28</sup> R. Merlin, cond-mat/0406275.

<sup>29</sup> C. Caroli, R. Combescot, P. Nozieres and D. Saint-James, *J. Phys. C: Solid St. Phys.* **4**, 916 (1971); *ibid.* **5**, 21 (1972).